International Journal of Thermal Sciences 48 (2009) 2119–2129

Contents lists available at ScienceDirect

International Journal of Thermal Sciences

journal homepage: www.elsevier.com/locate/ijts

Numerical study of developing laminar forced convection of a nanofluid in an annulus

M. Izadi [a], A. Behzadmehr [b,*], D. Jalali-Vahida [a]

[a] Mechanical Engineering Department, Sahand University of Technology, P.O. Box 51335-1996, Tabriz, Iran
[b] Mechanical Engineering Department, University of Sistan and Baluchestan, P.O. Box 98164-161, Zahedan, Iran

ARTICLE INFO

Article history:
Received 26 September 2008
Received in revised form
7 April 2009
Accepted 8 April 2009
Available online 12 May 2009

Keywords:
Nanofluid
Laminar forced convection
Annulus
Heat transfer enhancement

ABSTRACT

Laminar forced convection of a nanofluid consisting of Al_2O_3 and water has been studied numerically. Two dimensional elliptical governing equations have been solved to investigate the hydrodynamics and thermal behaviors of the fluid flow throughout an annulus. Single phase approach is used for the nanofluid modeling. The velocity and temperature profiles are presented in the fully developed region. The axial evolution of temperature, convective heat transfer coefficient and the friction coefficient at the inner and outer walls' region are shown and discussed. It is shown that the dimensionless axial velocity profile does not significantly change with the nanoparticle volume fraction. But, the temperature profiles are affected by the nanoparticle concentration. In general convective heat transfer coefficient increases with nanoparticle concentration. However, when the order of magnitude of heating energy is much higher than the momentum energy the friction coefficient depends on the nanoparticle concentration. At higher Reynolds numbers for which the momentum energy increases, this dependency on the nanoparticle volume fraction decreases.

1. Introduction

Nowadays after a century of struggling for enhancing industrial heat transfer by fluid mechanics, the low thermal conductivity of conventional fluids such as water, oil, and Ethylene-Glycol (EG) for transferring the heat has been one of the great challenges on the heat transfer science. One of the ways to overcome this problem is to replace conventional fluids with some advanced fluids with higher thermal conductivities. Maxwell's study in 1873 [1] shows the possibility of increasing the thermal conductivity of a fluid–solid mixture by increasing volume fraction of solid particles. Thus, the particles with micrometer or even millimeter dimensions were used. Those particles caused several problems such as abrasion, clogging and pressure losses.

During the past decade technology to make particles in nanometer dimensions was improved and a new kind of solid–liquid mixture that is called nanofluid, was appeared [2]. The nanofluid is an advance kind of fluid containing small quantity of nanoparticles (usually less than 100 nm) that are uniformly and stably suspended in a liquid. The dispersion of a small amount of solid nanoparticles in conventional fluids such as water or EG changes their thermal conductivity remarkably.

Thermal conductivity of nanofluids has been measured by several authors with different nanoparticle volume fraction, material and dimension in several base fluids and all findings show that thermal conductivity of nanofluid is higher than the base fluids. Among them, Lee et al. [3] demonstrated that oxide ceramic nanofluids consisting of CuO or Al_2O_3 nanoparticles in water or ethylene-glycol exhibit enhanced thermal conductivity. For example, using Al_2O_3 nanoparticles having mean diameter of 13 nm at 4.3% volume fraction increase the thermal conductivity of water under stationary conditions by 30% [4]. On the other hand, larger particles with an average diameter of 40 nm led an increase of less than 10% [3]. Different concepts have been proposed to explain this enhancement in heat transfer. Xuan and Li [5] and Xuan and Roetzel [6] have identified two causes of improved heat transfer by nanofluids: the increased thermal dispersion due to the chaotic movement of nanoparticles that accelerates energy exchanges in the fluid and the enhanced thermal conductivity of nanofluid. On the other hand, Keblinski et al. [7] have studied four possible mechanisms that contribute to the increase in nanofluid heat transfer: Brownian motion of the particles, molecular-level layering of the liquid/particles interface, ballistic heat transfer in the nanoparticles and nanoparticles clustering. Similarly to Wang et al. [8], they showed that the effects of the interface layering of liquid molecules and nanoparticles clustering could provide paths for rapid heat transfer.

* Corresponding author. Tel.: +98 541 2446251; fax: +98 541 2447092.
E-mail address: amin.behzadmehr@eng.usb.ac.ir (A. Behzadmehr).

1290-0729/$ – see front matter © 2009 Elsevier Masson SAS. All rights reserved.
doi:10.1016/j.ijthermalsci.2009.04.003

Nomenclature

B_c	Boltzman constant (J/K)
C	Specific heat (J/kg K)
C_f	Area average friction coefficient ($= \tau_i A_i + \tau_o A_o/A_i + A_o/(\rho V_0^2/2)$)
d_p	Nanoparticle diameter (nm)
d_f	Molecular diameter of base fluid (nm)
f_p	Friction coefficient
h_i	Inner wall convective heat transfer coefficient (W/m^2 K)
h_o	Outer wall convective heat transfer coefficient (W/m^2 K)
k	Thermal conductivity(W/m K)
L_{Bf}	Mean free path of base fluid (m)
N_i	Inner wall Nusselt number
N_o	Outer wall Nusselt number
P	Pressure (Pa)
Pr	Prandtl number
q_w	Uniform heat flux (W/m^2)
r	Radius (m)
Re	Reynolds number
T	Temperature (K)
V	Velocity (m/s)
x	Axial direction

Greek letter

ϕ	Volume fraction
μ	Dynamic viscosity ($N\,s/m^2$)
ρ	Density (kg/m^3)

Subscripts

app	appearance
eff	effective
f	base fluid
i	inlet
m	mixture
mr	mixture in radial direction
mx	mixture in axial direction
o	outlet
p	particle
s	solid
w	wall
wi	inner wall
wo	outer wall

Numerous theoretical and experimental studies have been conducted to determine the effective thermal conductivity of nanofluids. However, studies show that the measured thermal conductivity of nanofluid is much larger than the theoretical predictions [9,10]. Many attempts have been made to formulate efficient theoretical models for the prediction of the effective thermal conductivity [11–15]. Chon et al. [14] reported an experimental correlation for the thermal conductivity of Al_2O_3 as a function of nanoparticle size and fluid temperature. They showed that the Brownian motion of nanoparticle constitutes a key mechanism of the thermal conductivity enhancement with increasing temperature and decreasing nanoparticle size.

Nanoparticle high contact surface in comparison with larger particles, not only causes to improve heat transfer ability but also increases stability [4]. Xuan and Li [5] compared two kinds of nanofluid that one consisted in copper nanoparticles with 100 nm in diameter, and other consisted in copper nanoparticles with 10 nm in diameter. They showed that thermal conductivity of nanofluid, which included smaller particles, is higher than the one, which is made by the larger particles. This is also confirmed with the recent works of Li and Peterson [16] and Mints et al. [17]. They showed that the thermal conductivity enhancement of the two nanofluids demonstrated a nonlinear relationship with respect to temperature, nanoparticle volume fraction, and nanoparticle size. In addition they found the importance of the nanoparticle size on the effective thermal conductivity.

During the past decade many researchers have been started to study the hydrodynamic and thermal behaviors of various nanofluids at different flow conditions and also at different geometrical configurations numerically and experimentally. Among them Pak and Cho [18] and Xuan and Li [5,19] experimentally worked on convective heat transfer for laminar and turbulent flow of a nanofluid inside a tube. They introduced the first empirical correlations for the Nusselt number using nanofluids composed of water/Cu, water/TiO_2 and water/Al_2O_3. Ulzie et al. [20] studied laminar convective heat transfer and viscous pressure loss for alumina-water nanofluid in a vertical heated tube. Li and Kleinstreuer [21] studied the thermal performance of nanofluid flow in a trapezoidal microchannel. They showed that nanofluids do measurably enhance the thermal performance of microchannel mixture flow with a small increase in pumping power. Specifically, the thermal performance increases with volume fraction, but the extra pressure drop, will somewhat decrease the beneficial effects. Santra et al. [22] investigated the effect of copper–water nanofluid as a cooling medium to simulate the behavior of heat transfer due to laminar natural convection in a differentially heated square cavity. They observed that the heat transfer decreases with increase in the nanoparticle volume fraction for a particular *Ra*, while it increases with *Ra* for a particular nanoparticle volume fraction. Mirmasoumi and Behzadmehr [23] have studied the effects of nanoparticle mean diameter on the heat transfer and flow behavior into a horizontal tube under laminar mixed convection condition. Their calculated results demonstrate that the convection heat transfer coefficient significantly increases with decreasing the nanoparticles means diameter. However, the hydrodynamics parameters are not significantly changed. They also showed that the non-uniformity of the particles distribution augments when using larger nanoparticles and/or considering relatively high value of the Grashof numbers.

An appraisal of thermal augmentation of thermoelectric module using nanofluid-based heat exchanger is presented by Nnanna et al. [24]. They showed that there exist a lag-time in thermal response between the module and the heat exchanger. This is attributed to thermal contact resistance between the two components.

Numerical calculation of nanofluid convective heat transfer has been done in general with two different approaches; single phase or two-phase approach. The first one assumes that the fluid phase and nanoparticles are in thermal and hydrodynamic equilibrium. This approach is simpler and requires less computational time. Thus, several theoretical studies of convective heat transfer with nanofluids [25–29] used this approach. However, as mentioned by Ding and Wen [30] the distribution of the nanoparticles could only be assumed uniform if the corresponding Peclet numbers is always less than 10.

Annulus appears in many industrial heat exchangers. Therefore, many investigations have been done on the heat transfer mechanisms of an annulus. Among them Srivastava et al. [31] experimentally investigated the effect of an unheated length and the annulus ratio on the variations in heat transfer coefficient in the

early entrance region of an annulus. They showed that the effect of the shape of unheated section only becomes significant within x/D = 2. However, thereafter the results correspond to the fully developed condition.

Gupta and Garg [32] numerically studied laminar flow in the hydrodynamic entrance region of an annular tube by using an implicit finite difference. They found that for a very small annulus ratio the results depart significantly from those for a circular pipe. El-Shaarawiy and Alkam [33] solved numerically the transient laminar forced convection in the entrance region of an annulus. For different initial thermal conditions, they found that generally the responses associated with heating the outer boundary are more pronounced than those associated with heating the inner boundary are. Recently Lu and Wang [34] experimentally studied the convective heat transfer of water flow in a narrow annulus. They showed that the thermal characteristics of fluid flow in an annulus are different from those in circular tubes. Transition from laminar to turbulent occurs at the lower Reynolds number compared to the one for circular tubes. As seen in these and/or similar works, heat transfer mechanisms in annulus could be very complex and this geometry could be appeared in many industrial installation. Therefore, the present work aims to investigate some behaviors of nanofluid flow into such a geometrical configuration. Thus, the effects of nanoparticles volume fraction on the thermodynamics and hydrodynamics parameters of a laminar forced convection throughout an annulus have been studied.

2. Mathematical modeling

Laminar forced convection of a nanofluid consisting of water and Al_2O_3 in a horizontal annulus with uniform heat flux at the solid–liquid interfaces has been considered.

Fig. 1 shows the geometry of the considered problem. Because of symmetry, only one half of the geometry is considered for simulation. The effective viscosity and effective thermal conductivity of the fluid are considered a function of temperature. Dissipation and pressure work are neglected. In order to be able using single phase approach, ultrafine (<100 nm) solid particles are considered. Due to their non sediment nature, behaves as single phase fluid for which the fluid phase and nanoparticles are in thermal equilibrium

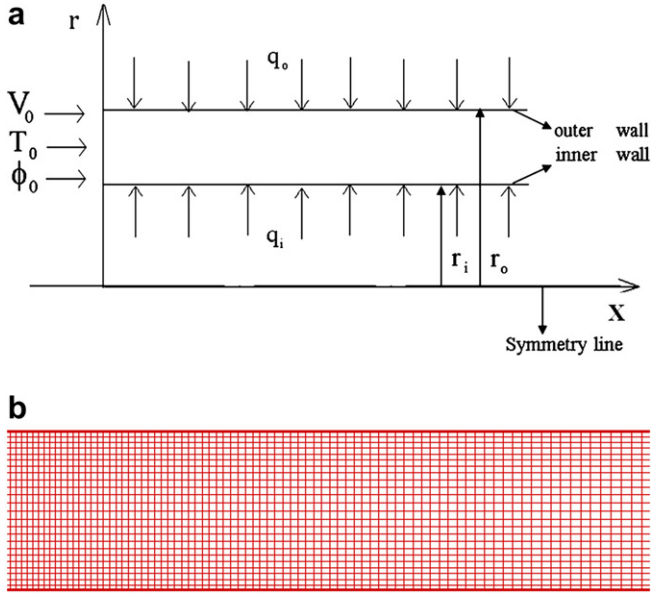

Fig. 1. (a) Schematic of the considered problem, (b) Grids distributions.

with zero relative velocity [35,36]. Therefore single phase approach is adopted for nanofluid modeling. With these assumptions the dimensional conservation equations for steady state mean conditions are as follows:Continuity equation:

$$\nabla\cdot\left(\rho_{\mathrm{eff}}V_{\mathrm{m}}\right) = 0 \tag{1}$$

Momentum equation:

$$\nabla\cdot\left(\rho_{\mathrm{eff}}V_{\mathrm{m}}V_{\mathrm{m}}\right) = -\nabla p + \nabla\cdot\left(\mu_{\mathrm{eff}}\nabla V_{\mathrm{m}}\right) \tag{2}$$

Energy equation:

$$\nabla\cdot\left(\rho_{\mathrm{eff}}CV_{\mathrm{m}}T\right) = \nabla\cdot\left(k_{\mathrm{eff}}\nabla T\right) \tag{3}$$

The physical properties of above equation are:

$$\rho_{\mathrm{eff}} = (1-\phi)\rho_{\mathrm{f}} + \phi\rho_{\mathrm{p}} \tag{4}$$

An accurate equation is used for calculating the effective heat capacitance [37].

$$C_{\mathrm{eff}} = \frac{(1-\phi)\rho_{\mathrm{f}}C_{\mathrm{f}} + \phi\rho_{\mathrm{p}}C_{\mathrm{p}}}{\rho_{\mathrm{eff}}} \tag{5}$$

Chon et al. [14] correlation, which considers the Brownian motion and mean diameter of the nanoparticles, has been used for calculating the effective thermal conductivity

$$\frac{k_{\mathrm{eff}}}{k_{\mathrm{f}}} = 1 + 64.7\times\phi^{0.7460}\left(\frac{d_{\mathrm{f}}}{d_{\mathrm{p}}}\right)^{0.3690}\left(\frac{k_{\mathrm{s}}}{k_{\mathrm{f}}}\right)^{0.7476}\times Pr^{0.9955}\times Re^{1.2321} \tag{6}$$

Where *Pr* and *Re* in Eq. (6) are defined as

$$Pr = \frac{\mu}{\rho_{\mathrm{f}}\alpha_{\mathrm{f}}} \tag{7}$$

$$Re = \frac{\rho_{\mathrm{f}}B_{\mathrm{c}}T}{3\pi\mu^2 l_{\mathrm{BF}}} \tag{8}$$

l_{BF} is the mean free path of water, $B_{\mathrm{c}}$is Boltzman constant ($B_{\mathrm{c}} = 1.3807\times10^{-23}$ J/K) and is calculated by the following equation:

$$\mu = A\times10^{\frac{B}{T-c}},\quad C = 140,\quad B = 247,\quad A = 2.414e-5 \tag{9}$$

Recently Masoumi et al. [38] developed a new equation for prediction of the nanofluids effective viscosity that is a function of temperature, mean nanoparticle diameter, nanoparticle volume fraction, nanoparticle density and the based fluid physical properties. This equation is adopted for calculating nanofluid effective viscosity:

$$\mu_{\mathrm{eff}} = \mu_{\mathrm{bf}} + \mu_{\mathrm{app}} \tag{10}$$

Where μ_{bf} and μ_{app} are base fluid and apparent viscosity respectively. Apparent viscosity is defined by:

$$\mu_{\mathrm{app}} = \frac{\rho_{\mathrm{p}}\nu_{\mathrm{B}}d_{\mathrm{p}}^2}{72\delta C} \tag{11}$$

where *C* depends on the base fluid viscosity and mean diameter of the nanoparticles, δ depends on mean diameter and volume fractions of the nanoparticles and ν_{B} is the Brownian velocity of nanoparticles that depends on temperature, diameter and density of particles.

$$C = \mu_{bf}^{-1}\left[(c_1 d_p + c_2)\phi + (c_3 d_p + c_4)\right] \quad (12)$$

where, $c_1 = -0.000001133$, $c_2 = -0.000002771$, $c_3 = 0.00000009$, $c_4 = -0.000000393$.

2.1. Boundary condition

This set of nonlinear elliptical governing equations has been solved subject to following boundary conditions:

- At the inlet of annulus ($X = 0$):

$$V_{mx} = V_i,\ V_{mr} = 0 \text{ and } T = T_i \quad (13)$$

- At the solid–fluid interfaces ($r = r_0$, $r = r_i$)

$$V_{mx} = V_{mr} = 0,\ \text{at } r = r_i\left(-k_{eff}\frac{\partial T}{\partial r}\right)_i = q_{wi} \text{ and at } r = r_0\left(-k_{eff}\frac{\partial T}{\partial r}\right)_o = q_{wo} \quad (14)$$

- At the annulus outlet ($X = L$): the diffusion flux in the direction normal to the exit plane is assumed to be zero for all variables except for the temperature that is considered to be fully developed at the tube outlet. An overall mass flux balance is also applied to correct velocities at outlet that are used for correcting the pressure.

2.2. Numerical method and validation

This set of nonlinear differential equation was discretized with the control volume technique. For the convective and diffusive terms, a first order upwind method was used while the SIMPLE procedure was introduced for the velocity-pressure coupling. The discretization grid is non-uniform in the radial and axial directions. It is finer near the tube entrance and near the wall where the velocity and temperature gradients are large. Several different grid distributions have been tested to ensure that the calculated results are grid independent. The selected grid for the present calculations consists of 250 and 25 nodes respectively in the axial and radial directions. Fig. 2 shows the radial variations of the velocity, temperature profile, axial evolution of the friction coefficient as well as convective heat transfer coefficient at different grids.

In order to demonstrate the validity and precision of the model and numerical procedure, comparisons with the available experimental and numerical simulation have also been done. Fig. 3 shows the comparison of the calculated results with the experimental results of Lu and Wang [34] in a narrow annulus. As it is shown the predicted friction factor ($f_p = 2d/l\Delta p/\rho v^2$) at different Reynolds number is in good agreement with the experimental results. In addition dimensionless fully developed velocity profile, the fully developed outer wall and inner wall Nusselt number are compared with the corresponding analytical results of Keys et al. [39]. As seen in Figs. 4–6 the concordance between the results is good. Therefore, the numerical code is reliable and can predict forced convection flow in a horizontal annulus.

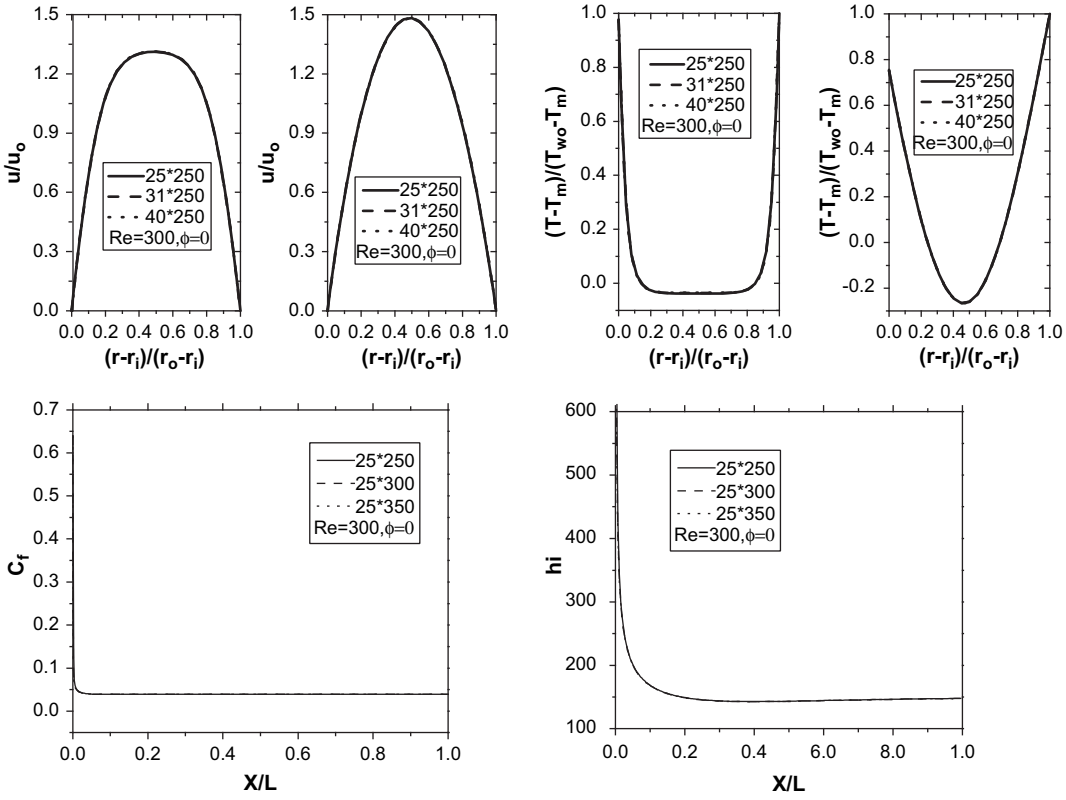

Fig. 2. Grid independence tests.

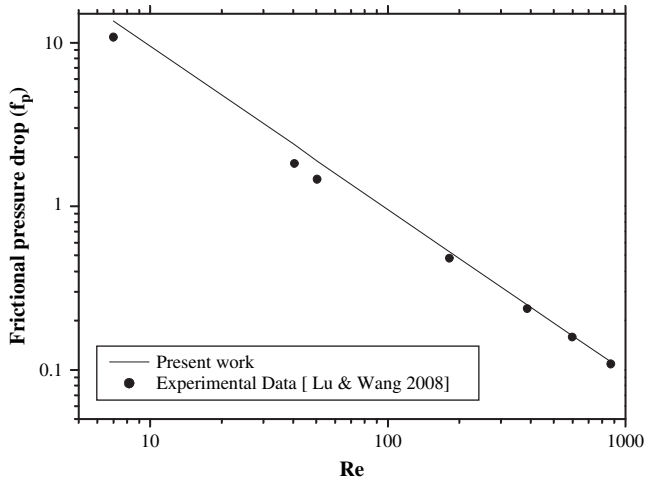

Fig. 3. Comparison of the predicted frictional pressure with the experimental results.

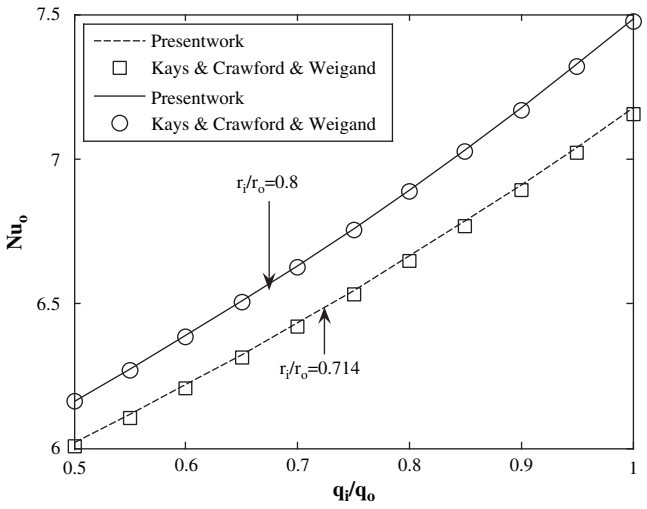

Fig. 5. Comparison of the predicted *Nu* at the outer wall with the analytical solution ($Re = 100$).

3. Results and discussion

Numerical simulations have been performed over a wide range of *Re*, particle volume fraction, wall heat flux and particle diameters. The results in this paper are presented at $Re = 100$ and 900, for different particles volume fractions (0%, 1%, 3%, 5%) with 25 nm mean diameter (spherical shape) and two different heat fluxes ratios.

Dimensional and dimensionless axial velocity profiles at the fully developed region are presented in Fig. 7. As it is seen dimensional axial velocity increases with nanoparticles volume fractions. This arises from the fact that the physical properties of nanofluid changes with the volume fraction. Therefore, different mean velocity is needed for different nanoparticle volume fraction to Reynolds number remains constant. However the dimensionless velocity profile shows no differences. This shows that despite different mean axial velocity at the tube entrance for different nanoparticle volume fraction (to have a constant *Re*) the dimensionless velocity profile remains constant and nanoparticle volume fraction does not have significant effect on the velocity profile. This behavior is also seen at the entrance region. While the effect of nanoparticle concentration on the temperature profile is significant. For instance, Fig. 8 shows the radial variations of dimensionless temperature at different axial positions. As shown for a given *Re* and different heat fluxes at the inner and outer walls, increasing the nanoparticle volume fraction changes the dimensionless temperature profile. It becomes to be more uniform which means more energy transfers through the fluid. It is known that the outer wall temperature is higher than the inner wall temperature. For the dimensionless radius less than 0.65, the dimensionless temperature of the nanofluid is larger than the base fluids. Because more energy transfers from the outer wall region to the inner wall region with using nanoparticles concentration ($T_{wi} < T_{wo}$). While at the dimensionless radius more than 0.65, the dimensionless temperature of the nanofluid is lower than the base fluids. This shows that the pure water ($\phi = 0$) could not transfer heating energy as it is done with nanofluids and therefore energy is accumulated at this region (region of the higher temperature). To see the effect of different heat fluxes at the inner and outer walls, axial evolution of the wall temperatures and also the bulk temperature for a given nanoparticle concentration are presented in Fig. 9. The interesting

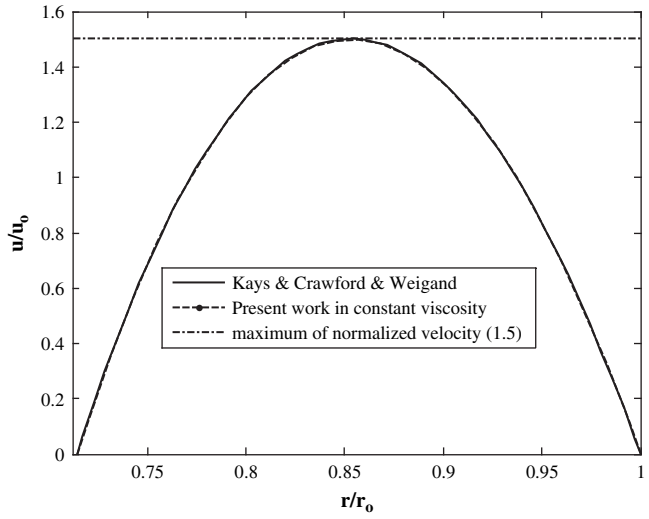

Fig. 4. Comparison of the predicted velocity profile with the analytical solution.

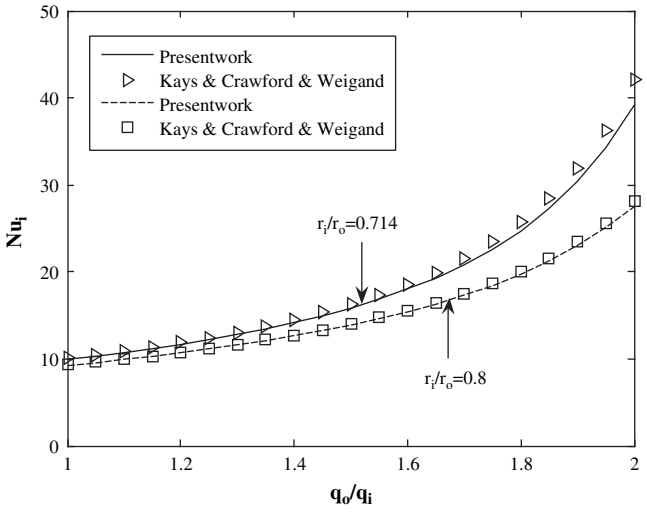

Fig. 6. Comparison of the predicted *Nu* at the inner wall with the analytical solution ($Re = 100$).

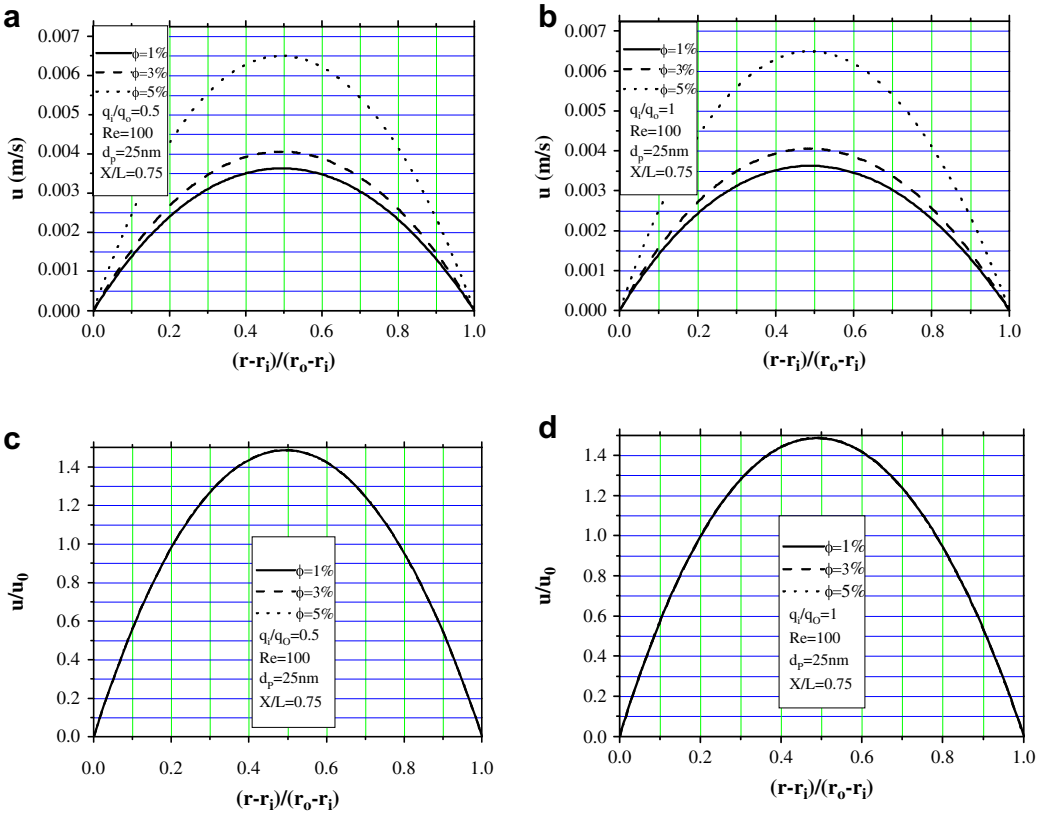

Fig. 7. Dimensional and dimensionless fully developed velocity profile.

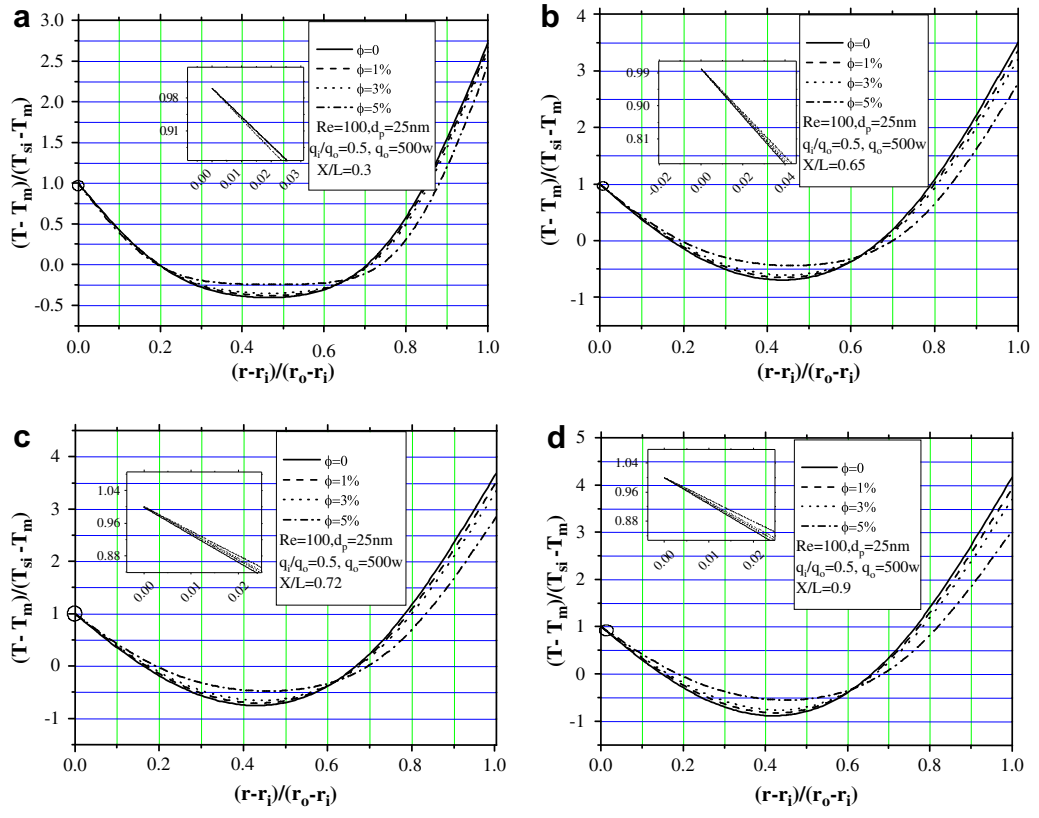

Fig. 8. Dimensionless temperature profile at different axial positions.

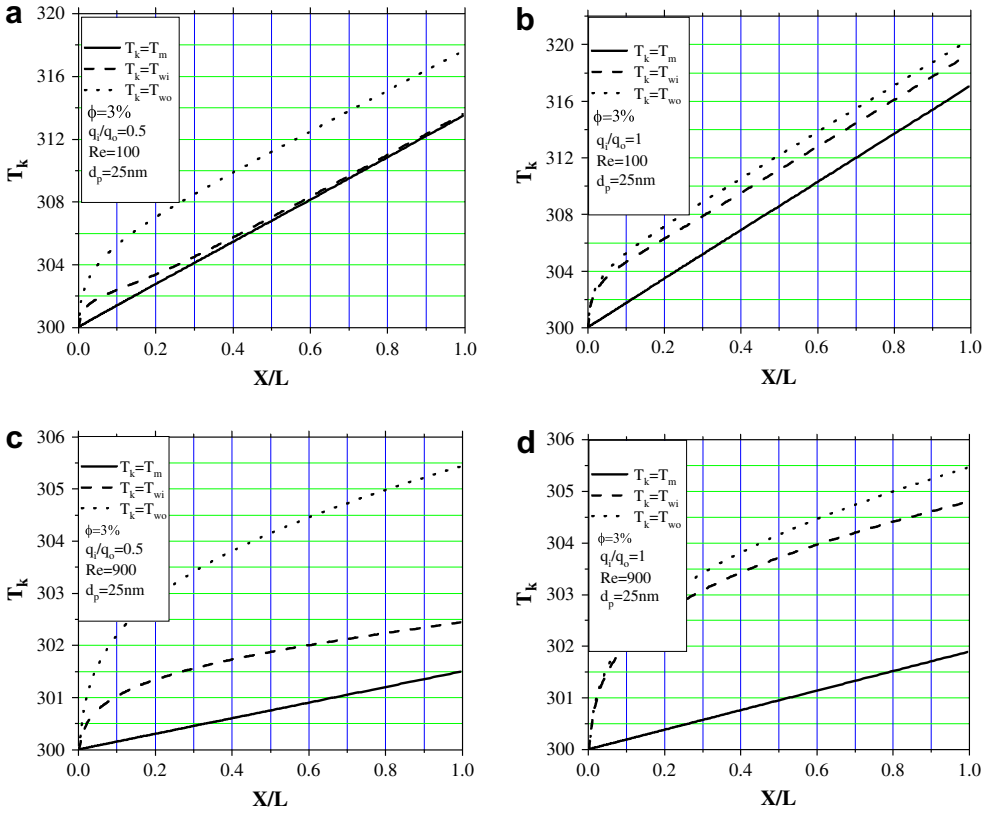

Fig. 9. Axial evolution of dimensional bulk and walls temperature.

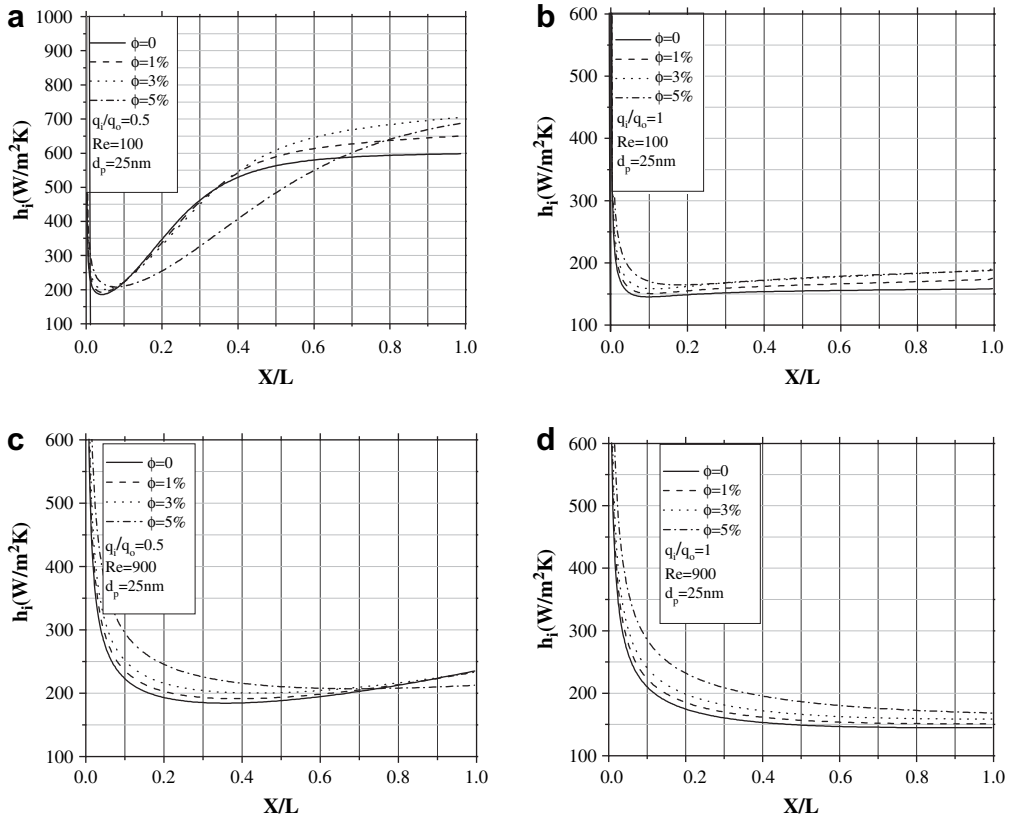

Fig. 10. Axial evolution of convective heat transfer coefficient at the inner wall (W/m^2 K).

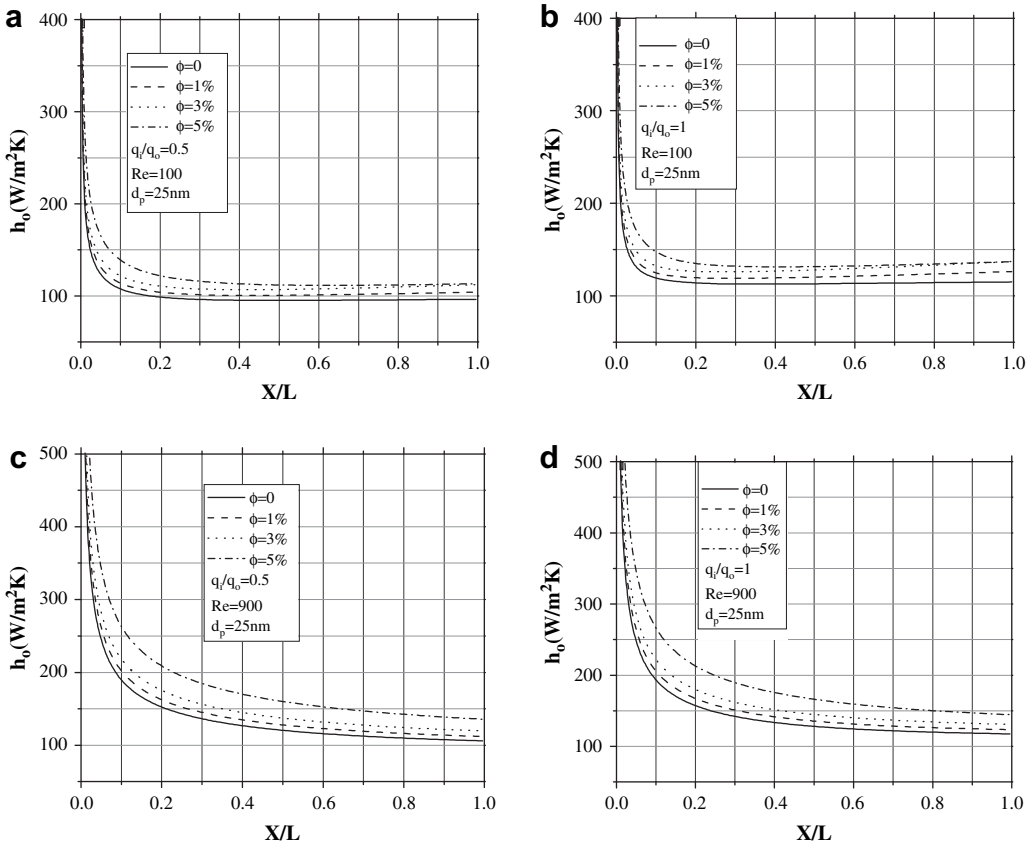

Fig. 11. Axial evolution of convective heat transfer coefficient at the outer wall (W/m^2 K).

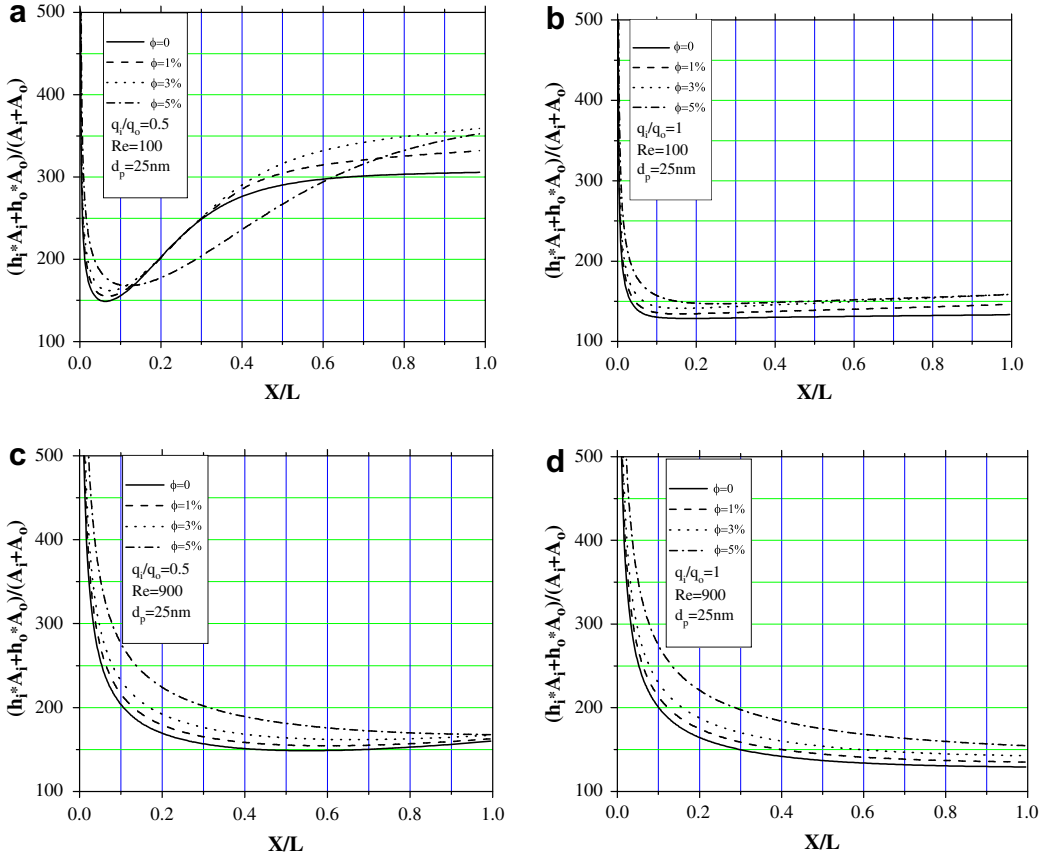

Fig. 12. Axial evolution of area average of convective heat transfer coefficient.

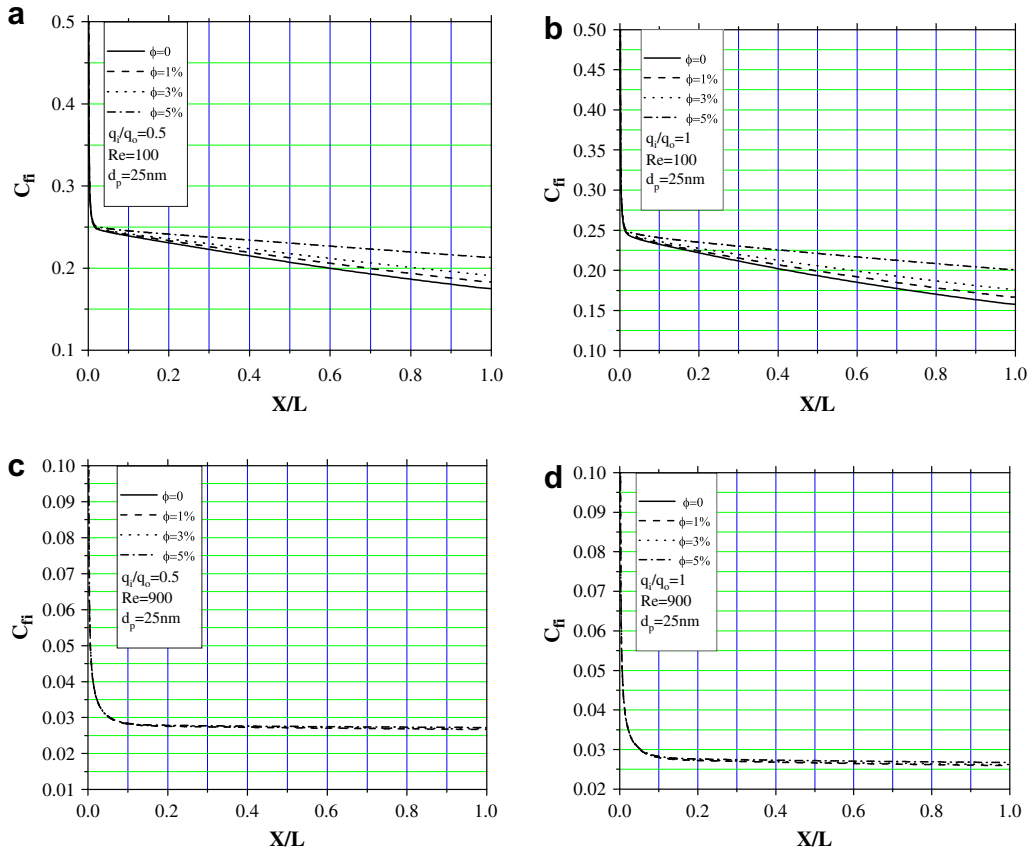

Fig. 13. Axial evolution of friction coefficient at the inner wall.

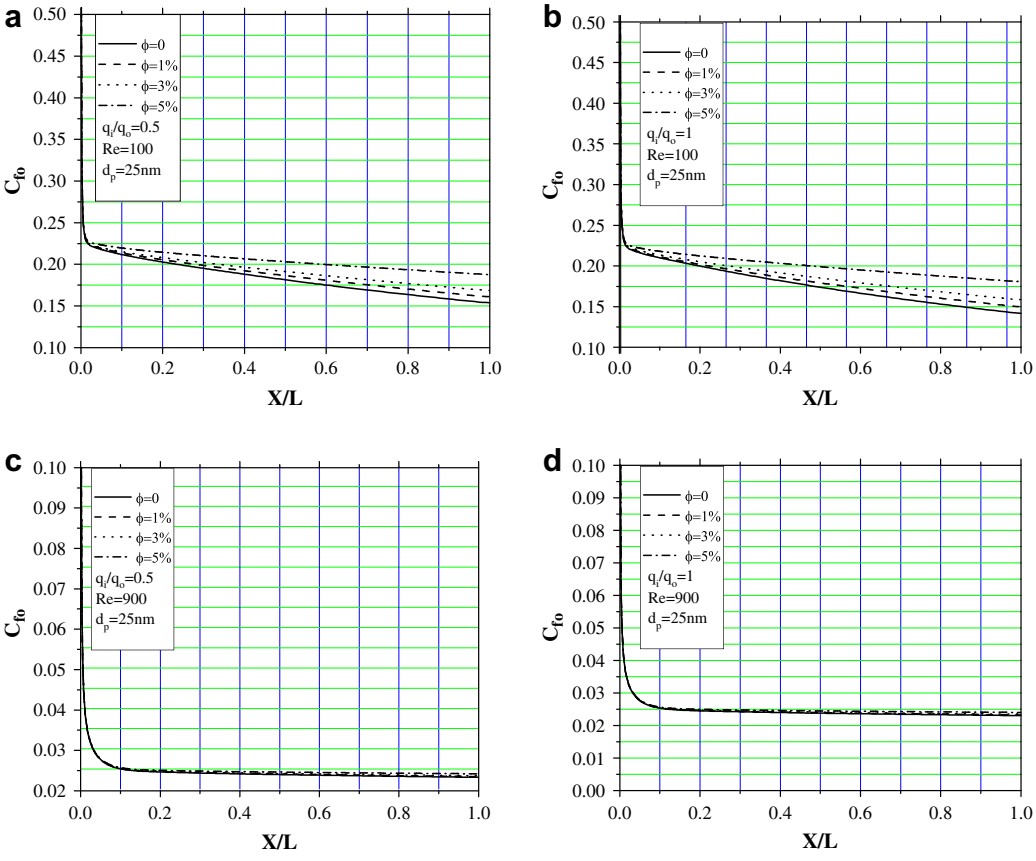

Fig. 14. Axial evolution of friction coefficient at the outer wall.

behavior is seen on the bulk temperature. Since the heat flux at the inner and outer walls is different, the wall temperature at these two walls are also different. While the fluid bulk temperature is resulted from these two different heat sources. Thus the fluid bulk temperature is higher than the situation for which the outer wall would be adiabatic or be at the same temperature as the inner wall is. As seen the bulk temperature is very close to the inner wall temperature when $q_i/q_o = 0.5$. However, increasing the inner wall heat flux to the value of the outer wall $q_i/q_o = 1$ (but the total heating energy at these two walls is different because of different area) increases the difference between the bulk and inner wall temperature. This effect on the bulk temperature could affect the calculated convective heat transfer coefficient at the inner wall. Axial evolution of the convective heat transfer coefficient at the inner and outer wall for two different *Re* and q_i/q_o are shown in Figs. 10 and 11. In general increasing the nanoparticle volume fraction increases the convective heat transfer coefficient at the fully developed region. However variation of the inner wall heat transfer coefficient at $Re = 100$ and $q_i/q_o = 0.5$ are not as it is usually seen (see Fig. 10a). This arises from definition of convective heat transfer coefficient that depends on the bulk temperature. As it was seen in Fig. 9 in such a situation, the bulk temperature becomes very close to the inner wall temperature. A negative effect of increasing nanoparticle volume fraction on h_i is observed for the higher Reynolds number ($Re = 900$) at the fully developed region. This may arise from the fact that in such a situation the order of magnitude of the momentum energy is much higher than the thermal energy. Therefore, the effect of increasing nanoparticle concentration on the thermal parameters decreases while a higher mass flow rate is needed for a given *Re* at higher nanoparticle volume fraction (because of variations of the nanofluid physical properties with the nanoparticles volume fractions). However, this variation is not seen in other cases for which the heating energy is higher. As it was mentioned, in general using nanofluid enhances the convective heat transfer coefficient. This is shown in Fig. 12 by the area average of convective heat transfer coefficient. Axial evolution of friction coefficients at the inner wall and outer wall are presented in Figs. 13 and 14. At the lower *Re*, increasing the nanoparticles volume fractions significantly augments the friction coefficient along the tube length. While it does not have an important effect at the higher Reynolds numbers. Because, for a given heat flux, at the high value of Reynolds number the variation of fluid temperature along the tube length are not significant and it could influence the variation of viscosity (viscosity consider as a function of temperature). The latter is the reason for important variation of friction coefficient at the low Reynolds number.

4. Conclusion

Laminar forced convection of a nanofluid consisting of Al_2O_3 and water has been studied numerically. It is shown that, for a given Reynolds number, despite changing the mean inlet velocity, the dimensionless velocity profile does not vary with nanoparticle volume fraction while the effect of nanoparticle concentration on the nanofluid bulk temperature is significant. In general using nanofluid with higher nanoparticle volume fraction increases the convective heat transfer coefficient. It is shown that by increasing the heat fluxes ratios (q_o/q_i), the effect of one wall heat flux on the *Nu* of another wall increases via its effects on the bulk temperature. However, the friction coefficient could increase when the order of magnitude of heating energy would be much higher than the momentum energy. At the higher Reynolds number for which the momentum energy increases this dependency on the nanoparticle volume fraction decreases.

References

[1] J.C. Maxwell, Electricity and Magnetism, Clarendon Press, Oxford, UK, 1873.
[2] S.U.S. Choi, Enhancing thermal conductivity of fluid with nanoparticles, developments and applications of non-Newtonian flow, ASME FED 231/MD 66 (1995) 99–105.
[3] S. Lee, S.U.S. Choi, S. Li, J.A. Eastman, Measuring thermal conductivity of fluids containing oxide nanoparticles, J. Heat Transf. 121 (1999) 280–289.
[4] H. Masuda, A. Ebata, K. Teramae, N. Hishinuma, Alteration of thermal conductivity and viscosity of liquid by dispersing ultra-fine particles (dispersions of -Al2O3, SiO2, and TiO2 ultra-fine particles), Netsu Bussei (Japan) 4 (1993) 227–233.
[5] Y.M. Xuan, Q. Li, Heat transfer enhancement of nanofluids, Int. J. Heat Fluid Flow 21 (2000) 58–64.
[6] Y.M. Xuan, W. Roetzel, Conceptions for heat transfer correlation of nanofluids, Int. J. Heat Mass Transf. 43 (2000) 3701–3707.
[7] P. Keblinski, S.R. Phillpot, S.U.S. Choi, J.A. Eastman, Mechanisms of heat flow in suspensions of nano-sized particles (nanofluid), Int. J. Heat Mass Transf. 45 (2002) 855–863.
[8] X. Wang, X. Xu, S.U.S. Choi, Thermal conductivity of nanoparticle-fluid mixture, J. Thermophys. Heat Transf. 13 (1999) 474–480.
[9] S.U.S. Choi, Z.G. Zhang, W. Yu, F.E. Lockwood, E.A. Grulke, Anomalous thermal conductivity enhancement in nanotube suspensions, Appl. Phys. Lett. 79 (2001) 2252–2254.
[10] X. Zhang, H. Gu, M. Fujii, Effective thermal conductivity and thermal diffusivity of nanofluids containing spherical and cylindrical nanoparticles, Exp. Therm. Fluid Sci. 31 (2007) 593–599.
[11] Q.Z. Xue, Model for effective thermal conductivity of nanofluids, Phys. Lett. A 307 (2003) 313–317.
[12] Y.M. Xuan, Q. Li, W. Hu, Aggregation structure and thermal conductivity of nanofluids, AIChE J. 49 (2003) 1038–1043.
[13] S.P. Jang, S. Choi, Role of Brownian motion in the enhanced thermal conductivity of nanofluids, Appl. Phys. Lett. 84 (2004) 4316–4318.
[14] C.H. Chon, K.D. Kihm, S.P. Lee, S.U.S. Choi, Empirical correlation finding the role of temperature and particle size for nanofluid (Al_2O_3) thermal conductivity enhancement, Appl. Phys. Lett. 87 (2005) 1–3.
[15] N. Sohrabi, Modeling effective thermal conductivity coefficient of nanofluids using two phase model. MSc Thesis, University of Sistan and Baluchestan, 2008.
[16] C.H. Li, G.P. Peterson, The effect of particles size on the effective thermal conductivity of Al_2O_3-water nanofluids, J. Appl. Phys. 101 (2007) 044312.
[17] H.A. Mintsa, G. Roy, C.T. Nguyen, D. Doucet, New temperature dependent thermal conductivity data for water based nanofluids, Int. J. Therm. Sci. 48 (2009) 363–371.
[18] B.C. Pak, Y.I. Cho, Hydrodynamic and heat transfer study of dispersed fluids with submicron metallic oxide particles, Exp. Heat Transf. 11 (1998) 151–170.
[19] Y.M. Xuan, Q. Li, Investigation on convective heat transfer and flow features of nanofluids, J. Heat Transf. 125 (2003) 151–155.
[20] U. Rea, T. McKrell, L. Hu, J. Buongiorno, Laminar convective heat transfer and viscous pressure loss of alumina–water and zirconia–water nanofluids. Int. J. Heat Mass Transf., doi:10.1016/j.ijheatmasstransfer. 2008.10.025.
[21] J. Li, C. Kleinstreuer, Thermal performance of nanofluid flow in microchannels, Int. J. Heat Fluid Flow 29 (2008) 1221–1232.
[22] A.K. Santra, N. Chakraborty, S. Sen, Prediction of heat transfer due to presence of copper–water nanofluid using resilient-propagation neural network. Int. G. Therm. Sci., doi:10.1016/j.ijthermalsci.2008.11.009.
[23] S. Mirmasoumi, A. Behzadmehr, Effect of nanoparticles mean diameter on mixed convection heat transfer of a nanofluid in a horizontal tube, Int. J. Heat Fluid Flow 29 (2008) 557–566.
[24] A.G.A. Nnanna, W. Rutherforda, W. Elomara, B. Sankowski, Assessment of thermoelectric module with nanofluid heat exchanger, Appl. Therm. Eng. 29 (2009) 491–500.
[25] C.T. Nguyen, G. Roy, C. Gauthier, N. Galanis, Heat transfer enhancement using Al_2O_3 water nanofluid for an electronic liquid cooling system, Appl. Therm. Eng. 27 (2007) 1501–1506.
[26] K. Khanafer, K. Vafai, M. Lightstone, Buoyancy-driven heat transfer enhancement in a two dimensional enclosure utilizing nanofluids, Int. J. Heat Mass Transf. 46 (2003) 3639–3653.
[27] J. Koo, C. Kleinstreuer, Laminar nanofluid flow in microheat-sinks, Int. J. Heat Mass Transf. 48 (2005) 2652–2661.
[28] M. Akbari, A. Behzadmehr, F. Shahraki, Fully developed mixed convection in horizontal and inclined tubes with uniform heat flux using nanofluid, Int. J. Heat Fluid Flow 29 (2008) 545–556.
[29] A. Akbarinia, A. Behzadmehr, Numerical study of laminar mixed convection of a nanofluid in a horizontal curved tube, Appl. Therm. Eng. 27 (2007) 1327–1337.
[30] Y. Ding, D. Wen, Particle migration in a flow of nanoparticle suspensions, Powder Technol. 149 (2005) 84–92.
[31] N.C. Srivastava, F. Bakhtar, F.K. Bannister, An investigation into thermal boundary layer growth in the entrance region of an annulus, Int. J. Heat Mass Transf. 14 (1973) 49–59.
[32] S.C. Gupta, V.K. Garg, Developing flow in a concentric annulus, Comput. Meth. Appl. Mech. 28 (1981) 27–35.
[33] M.A.I. El-Shaarawiy, M.K. Alkam, Transient forced convection in the entrance region of concentric annuli, Int. J. Heat Mass Transf. 35 (1992) 3335–3344.

[34] G. Lu, J. Wang, Experimental investigation on heat transfer characteristics of water flow in a narrow annulus, Appl. Therm. Eng. 28 (2008) 8–13.
[35] N. Putra, W. Roetzel, S.K. Das, Natural convection of nano fluids, J. Heat Mass Transf. 39 (2003) 775–784.
[36] W. Daungthongsuk, S. Wongwises, A critical review of convective heat transfer of nanofluids, Renew. Sustain. Energ. Rev. 11 (5) (2007) 797–817.
[37] S.Q. Zhou, R. Ni, Measurement of the specific heat capacity of water-based Al_2O_3 nanofluid, Appl. Phys. Lett. 92 (2008) 093123.
[38] N. Masoumi, N. Sohrabi, A. Behzadmehr, A new model for calculating the effective viscosity of nanofluids, J. Phys. D Appl. Phys. 42 (2009) 055501.
[39] W. Kays, M. Crawford, B. Weigand, Convective Heat and Mass Transfer, McGraw-Hill, 2004.